



Contents lists available at www.sciencedirect.com

Journal of the European Ceramic Society

journal homepage: www.elsevier.com/locate/jeurceramsoc



Rheological behaviour and thermal dilation effects of alumino-silicate adhesives intended for joining of high-temperature resistant sandwich structures

Martin Černý^{a,*}, Zdeněk Chlup^b, Adam Strachota^c, Jana Schweigstillová^a, Jaroslava Svítílová^a, Martina Halasová^b

^a Institute of Rock Structure and Mechanics of the Academy of Sciences of the Czech Republic, v.v.i., Prague, Czechia

^b Institute of Physics of Materials of the Academy of Sciences of the Czech Republic, v.v.i., Brno, Czechia

^c Institute of Macromolecular Chemistry of the Academy of Sciences of the Czech Republic, v.v.i., Prague, Czechia

ARTICLE INFO

Article history:

Received 4 August 2016

Received in revised form

22 December 2016

Accepted 26 December 2016

Available online xxx

Keywords:

Sandwich

Inorganic adhesive

Si–O–C ceramics

Ceramic foam

Ceramic fibre

ABSTRACT

The study is concerned with inorganic adhesive layers located between the CMC composite skin and the Si–O–C ceramic foam core of sandwiches intended for high-temperature use. Two types of alumino-silicate adhesives (mastics) were tested for use as the bonding layer. The rheological properties of adhesive and its dimensional changes during high-temperature curing play a key role in terms of successful manufacture and subsequent use at high temperatures. In order to characterise these properties, specimens consisting only of the dried adhesive were subjected to compression tests conducted at increasing temperature from 300 to 1000 °C. These experiments were carried out via the application of two loading modes using both the static pre-load and cyclic loading methods. The above results were compared with thermal expansion records determined from fully-cured adhesives. In addition to the above investigation, the mechanical properties of the adhesive joint were measured employing both the DCB and shear tests.

© 2016 Elsevier Ltd. All rights reserved.

1. Introduction

Sandwich structures consisting of refractory materials are potentially attractive for several industries, including aerospace and automotive [1]. Commonly used sandwich structures mainly provide considerable weight reduction, which is undoubtedly a great benefit. In the case of structures consisting exclusively of ceramic materials, such sandwiches offer an opportunity to resolve two additional important problems of advanced ceramics: First is the product price reduction by reducing the amount of very costly ceramic fibres which are used in the production of ceramic matrix composites (CMC). The second opportunity is more academic and involves the quest for improved fracture toughness and impact resistance of ceramics. Impact-resistant sandwich materials combining a polymer matrix laminate or metal with ceramics can be an inspiration for analogical solutions in the field of ceramic materials [2,3].

In view of the above facts, it is at first glance surprising, that sandwich structures consisting solely of ceramic materials are rarely discussed in scientific journals, in contrast to CMC which are still being further developed and which are being frequently discussed [4–17], similarly like ceramic foams [18–30] or porous ceramics [31–37]. The probable reason is, that the design and production of ceramic sandwich materials is quite a complicated problem, which requires the knowledge of several disciplines of materials sciences. In terms of structure, two basic varieties of ceramic sandwich core have been investigated: corrugated ceramic core [38] and ceramic foam core [39].

The interface between the ceramic core and the ceramic skin is a key problem for design and production of ceramic sandwiches. One possible solution is bonding with high-temperature inorganic adhesive. Joining of basic types of ceramics by using high-temperature adhesives is described e.g. in [40,41] for SiC and in [42,43] for Al₂O₃. High temperature inorganic adhesives for fixing of ceramics are currently often discussed in the context of solid oxide fuel cells, where they are used for joining the ceramic electrolyte with the frame of the fuel cell [44–56]. Unlike in case of structural sandwiches, the joints in fuel cells must be gas-tight. The operating temperatures of these joints reach up to 800 °C. Similar

* Corresponding author.

E-mail address: cerny@irsm.cas.cz (M. Černý).

Table 1

Properties of the Si–O–C foam obtained from the MPS precursor.

elemental composition	average pore size	bulk density	apparent density	elastic modulus	compressive strength
SiO _{1.4} C _{2.4}	0.41 mm	1.81 g cm ⁻³	0.43 g cm ⁻³	1.5 GPa	9.8 MPa

demands are placed on high-temperature adhesives for fixing and sealing of perovskite membranes [57].

Bonding of CMC skin on a ceramic foam core is a separate and very challenging task. The adhesive connection between skin and foam core must meet several essential requirements:

- 1) The thermal expansion of all components of the sandwiches should be as similar as possible throughout the whole temperature range of the intended use.
- 2) The thermal expansion of the binder during its high-temperature curing should differ as little as possible from the expansion curve of fully cured binder.
- 3) The cured binder should have good adhesion to the skin as well as to the core in the whole temperature range of the intended use.
- 4) The non-cured binder should have a certain adhesion to the core and to the skin in the entire range of the high-temperature curing during the production of the sandwich.
- 5) When using a foam core, the binder should fill to some extent the pores, in order to increase the adhesion area. For this reason, it is advisable to use mastics with optimal filler grain size as binder.
- 6) None of the sandwich components should be affected by creep in the entire temperature range of the intended use. In particular, this demand applies to the high-temperature adhesive.

The aim of our study is to present a development and production process of a ceramic sandwich structure, with special focus on dilation and on rheological behaviour of the inorganic adhesive during its high-temperature curing process. These properties were studied in several types of compression experiments, using either cyclic load or static pre-load in the range from 300 to 1000 °C. The strength of the adhesive bond was tested in double cantilever beam (DCB) and in shear tests.

2. Material

The material investigated in this study is a high-temperature sandwich intended for use up to 1000 °C. The face sheet layers (skins) are made of a ceramic matrix composite (CMC) with a matrix based on pyrolyzed polymethylsiloxane resin (MS). The sandwich core is formed by a Si–O–C foam, which was prepared by pyrolysis of the polymethylphenylsiloxane resin (MPS). The skins and the core are bonded by an alumino-silicate adhesive (alumino-silicate mastic).

2.1. Skins

As an outer supporting layer, two variants of the fabric-reinforced CMC which differed in fibre type were used. The first type was Nextel 720 – a fibre having the alumina-mullite nanocrystalline structure. The elastic modulus of these fibres is 190 GPa and its maximum service temperature is 1300 °C. The second type was Nextel 610 – a fibre with pure alumina nanocrystalline structure which possesses improved creep resistance, elastic modulus of 300 GPa and a maximum service temperature of 1400 °C. Both types of composites have been produced by manual lamination of woven satin fabric which has been impregnated with the polymethylsiloxane (MS) resin. Plate-shaped samples were moulded and cured at a temperature/pressure controlled mode (up to 0.8 MPa and 250 °C). Subsequently, the composite plates were pyrolyzed at a slow heat-

ing rate up to 1100 °C (from 20 to 250 °C with 50 °C/h and from 250 to 1100 °C with 20 °C/h, followed by a 6 h dwell time at this temperature).

Structural changes in the MS precursor resin during the pyrolysis are described in [58,59]. The composite reinforced with Nextel 720 fibres (hereinafter N720) has a strength of 58 MPa, Young's modulus of 66 GPa and apparent density of 2.24 g/cm³. The composite reinforced with Nextel 610 fibres (hereinafter N610) has a strength of 67 MPa, Young's modulus of 92 GPa and density of 2.45 g/cm³.

2.2. Core

The foam core of the sandwich was produced by foaming the polymethylphenylsiloxane (MPS) resin with 12 wt.% of added starch. Foaming and curing of the preceramic foam took place simultaneously at 230 °C for 2 h. Subsequently, the foam was pyrolyzed at a slow heating rate up to 1100 °C using same temperature program as in the case of the skin plates (see 2.1). This foam has good mechanical properties, combined with good oxidation resistance at high temperatures, and its amorphous structure displays a high thermal stability. The low density of this foam is the key advantage for the use in sandwich structures. The production process and the properties of the foam are described in [26] and in [28]. The basic properties of the used foam are summarized in Table 1.

2.3. The adhesive layers of the studied sandwich structure

As a binder between the skins and the foam core, two types of high-temperature adhesives based on alumino-silicate mastic, which differ in their technological properties, were used. These two adhesives were selected in preliminary experiments among the six initially studied inorganic binders.

The initial intention of the authors was to produce a sandwich during foaming and curing of the core, without any adhesive layer, but significant differences in the shrinkage of the foam core and of the composite skins during pyrolysis did not allow implementing this intention. Second possibility of skin/core joining is the use of MS or MPS resin as adhesive after completed pyrolysis of the CMC skins and of the foam core. However, this method does not provide sufficient bonding strength after the pyrolysis of the adhesive resin layer.

Gluing of Si–O–C foam core and CMC composite skin by alumino-silicate adhesive was found to be successful and the adhesive provides a strong bond even where the bonded surfaces are separated by some distance – for example in a pore. The adhesive, however, forms an autonomous region with a thickness between ca. 0.1 and 1 mm, and therefore it must be considered as a separate layer which, by its mechanical properties, affects the entire sandwich.

The alumino-silicate adhesive with the trade name HT Silicate Adhesive (hereinafter SA) produced by Techniqll (Poland) is designed for the use at temperatures up to 1200 °C. The composition determined by EDS is: 55 wt.% of SiO₂, 40 wt.% of Al₂O₃, 0.3 wt.% of Fe₂O₃ and 2.5 wt.% of Na₂O + K₂O. SA has a density of 2.22 g/cm³. The alumino-silicate adhesive Rudokit NT1350 (hereinafter Rk – the manufacturer uses the term “mastic”) produced by P-D Refractories CZ a.s. in the Czech Republic is certified for the use up to 1350 °C. The chemical composition provided by the man-

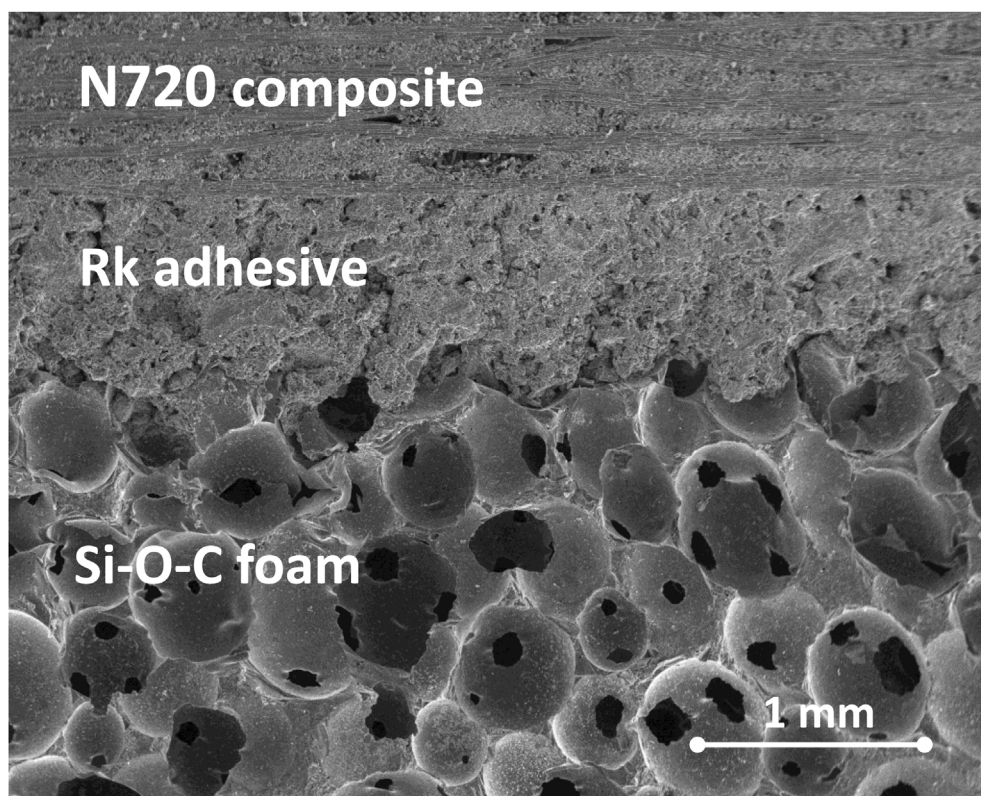


Fig. 1. Adhesive connection between the Si–O–C foam core and the CMC composite skin after high temperature curing at 1000 °C (SEM micrograph).

ufacturer is: 57 wt.% of SiO_2 , 38 wt.% of Al_2O_3 , 0.6 wt.% of Fe_2O_3 and 3.5 wt.% of $\text{Na}_2\text{O} + \text{K}_2\text{O}$. Rk has a density of 2.12 g/cm^3 . An important parameter is the maximum size of the filler particles, which in the case of SA is equal to 0.1 mm, and in the case of Rk is equal to 0.5 mm. If the mastic is used as an adhesive, then this parameter determines the minimum thickness of the adhesive layer. A deeper study of structural transformations, which occur during the high-temperature cure of the employed adhesives, is not a part of this work.

2.4. The preparation of the sandwich samples for the mechanical testing

The sandwich samples for the assessment of adhesion strength were prepared by gluing upper and lower skins on the pyrolysed foam core with the help of an alumino-silicate adhesive. Four variants were tested, using the mentioned two types of adhesive, i.e. Rk or SA, and two types of composite skins, i.e. N610 or N720. All of these sandwich variants were prepared in the same way: The adhesive was applied between the pyrolysed foam and composite skin plate in a layer of 0.3–1 mm thickness depending on the surface geometry and on the viscosity of untreated adhesive. The sandwich sample was subsequently dried for one day at room temperature. During drying, a strong hardening of the adhesives occurs, combined with a good adhesion to all surfaces of the glued components. Finally, the sandwich samples were annealed up to 1000 °C, at a heating rate of 2.5 °C/min. (hereinafter the 'high-temperature curing'). The structure of the bonded joints is shown in Figs. 1 and 2.

3. Experimental

Measurements of dilation and of changes in rheological properties during the high-temperature curing were performed on a standard testing machine Inspekt 100 (Hegewald & Peschke,

Germany), equipped with the testing furnace and with the high-temperature bending/compression jig "PMA-06/V6 Biege-Mess-Vorrichtung bis 1500 °C" (Maytec, Germany), using an independent extensometer. The precision of the high-temperature extensometer is $\pm 0.03 \mu\text{m}$. The above-mentioned jig was used in a configuration for compression testing. The experimental arrangement is shown in Fig. 3. The sample dimensions were $12 \text{ mm} \times 10 \text{ mm} \times 8 \text{ mm}$ (the gauge length for the determination of the dilations was 12 mm).

The DCB (double cantilever beam) and shear experiments were carried out by the universal testing machine MTS Tytron 250. The schemes of testing configurations are shown in Fig. 4. The applied cross-head speed was 0.1 mm/min . Nominal dimensions of DCB specimens prepared from sandwiches were $25 \text{ mm} \times 10 \text{ mm}$ in the joining plane (the skin size was $50 \text{ mm} \times 10 \text{ mm}$) and thickness of approximately 15 mm depending on the final adhesive thickness. Specimens for the shear test were the same like those for the DCB test, but without one skin/adhesive layer.

Scanning electron microscopy (SEM) was employed for the observation of the microstructure of the composites. A FEI Quanta 450 microscope was used, equipped with an ETD (detection of secondary electrons).

4. Results and discussion

4.1. Assessment of the thermally stabilized materials for the use in the sandwich structures in terms of thermal expansion

During the manufacture, as well as during the operational use of sandwich structures, considerable shear stresses arise due to different temperature expansion coefficients of skin, core and adhesive layers. The ideal situation would occur, if the thermal expansion coefficients of all the components of the sandwich had the same

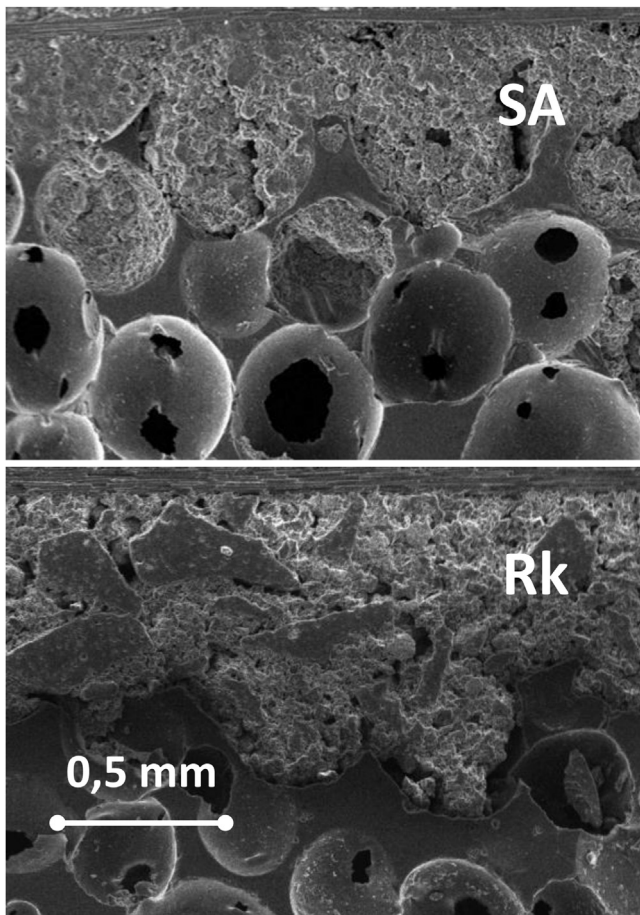


Fig. 2. The fine grain size of the unprocessed SA adhesive allows the formation of a thinner bonding layer and better filling of the pores; above SA adhesive, below Rk adhesive – both structures after high-temperature curing at 1000 °C (SEM micrograph).

value. This situation cannot be achieved because of the limited choice of available high-quality ceramic fibres.

The experimental results of the thermal expansion of thermally stabilised materials (in the case of adhesives: high-temperature curing up to 1000 °C with 1 h dwell at this temperature; in the case of skins and core materials: pyrolysis up to 1100 °C), which were used as components in the investigated sandwich structures are shown in Fig. 5. Both adhesives display a similar behaviour of thermal expansion like the composite materials used for sandwich skins. The N610 composite skin and the Rk adhesive exhibit almost an identical course. The thermal expansion of the N720 composite is somewhat lower, which is a result of different crystal structures of the fibres in N610 and in N720 composites.

Among the investigated components, the Si-O-C foam exhibits by far the lowest thermal expansion, with a coefficient lower than 2×10^{-6} . The difference between the thermal expansion coefficients of the foam core on one hand, and of the CMC skins and the cured adhesive on the other, could present a serious problem. However, a low elastic modulus of the foam still could allow for a proper function of the sandwich. If a simple sandwich model is considered, with mechanically non-deformable skins exhibiting thermal expansion and the foam exhibiting thermal expansion and elasticity, then the calculated compressive stress in the foam at 20 °C is 9 MPa, which is less than its compressive strength. This calculation assumes that a fully rigid connection between the skins and the core is formed at 1000 °C. If such a connection is formed at lower temperatures, the compressive stress will be lower. Phenomena like creep and vis-

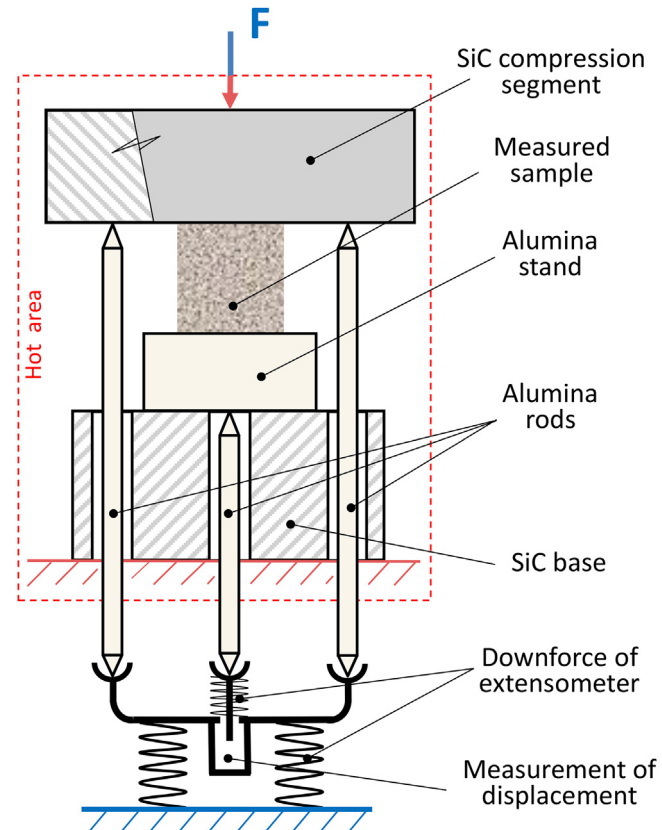


Fig. 3. Experimental setup for the characterization of the rheological behaviour and of the thermally induced dimensional changes of the studied adhesives.

coelasticity of the adhesive, which are known to occur, also further reduce the compressive stress in the foam (after cooling down to 20 °C).

4.2. The rheological behaviour and the thermally induced dimension changes in the adhesive during the high-temperature curing

4.2.1. Experimental approach for characterization of the high-temperature curing process

The mechanical properties and the thermal expansion of individual components of sandwiches in a thermally stable state (after completed pyrolysis or annealing) are not the only criteria for their suitability. During the production of the sandwiches, the adhesive is undergoing significant structural transformations and its creep and thermal expansions or shrinkages play a significant role. The below-described experiments show that these properties can decide about the preparation method suitable for a particular sandwich design.

The sandwich structure developed in this work assumes the use of the CMC composite skins moulded and pyrolysed separately from the other components of the sandwich. Also the production of the foam core is proceeding separately until pyrolysis. Both of these components are sufficiently thermally stabilized and thereby, during the subsequent sandwich preparation, their properties will not change (for details see literature [10,26,59]).

During the high-temperature curing, which follows after the initial bonding of the sandwich, the adhesive undergoes crucial structural transformations accompanied by significant changes in mechanical properties and in dimensions. For the assessment of these changes, three types of experiments were conducted: 1) a rheological characterization of the adhesive during the cure pro-

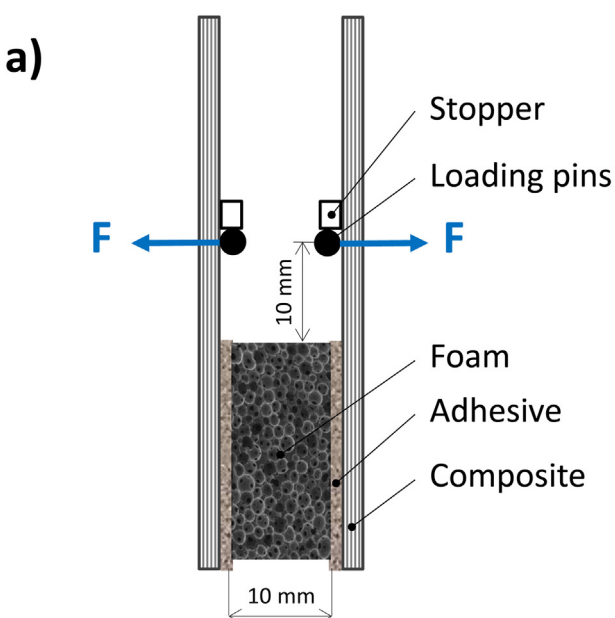


Fig. 4. Experimental setup for mechanical tests of adhesive bond between skin and core: a) modified DCB test and b) shear test.

cess, 2) measurement of adhesive dilation during the cure and 3) dilation measurement of the thermally stabilised adhesive.

High-temperature curing of an inorganic adhesive induces a variety of phenomena, such as hardening, softening (including creep and viscoelasticity), expansion or shrinkage. In some stages of the curing process, there is a high risk of cracks arising from excessive tensile loads or from uneven expansion or shrinkage. For these reasons, mechanical tests were carried out at a slow heating rate and at very low load and preload. Records of rheological/expansion characterization of alumino-silicate adhesives are shown in Figs. 6–9. These experiments were conducted up to 1000 °C. The loading cycle applied during the experiments consists of a preload of 5 N (≈ 0.05 MPa of compression in sample) lasting 300 seconds, which is followed by a linear increase to 30 N (≈ 0.3 MPa) and this load is held for 10 seconds. The cycle is finished by a linear descent to the original preload value. The measured

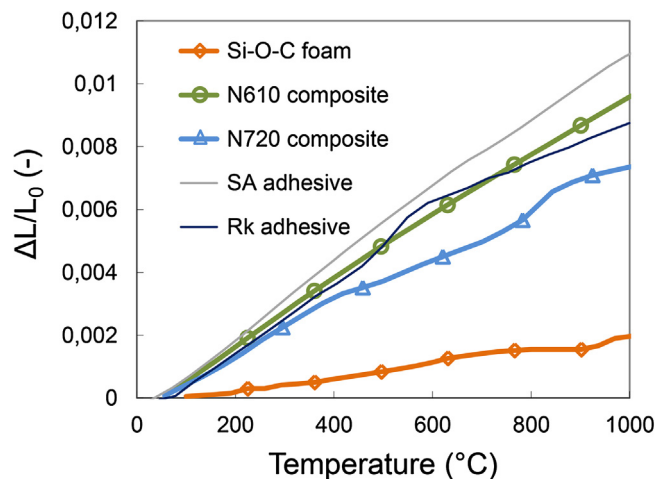


Fig. 5. Thermal dilations of alternatively used sandwich components in their thermally stabilised state (post-cure, post pyrolysis).

value of expansion $\Delta L/L_0$ at a given temperature during high-temperature cure and under cyclic loading is the sum of four fundamentally different components: the first component is the reversible thermal expansion, the second is dilation resulting from thermally induced structure changes, the third component is the creep deformation caused by the cyclic loading and by preload applied to the sample, and the fourth is viscoelastic deformation in response to the cyclic loading and preload. Among these four effects, the reversible thermal expansion always has a positive value, the dilation originating in structure changes can be positive or negative (expansion or shrinkage), while creep and viscoelastic deformation always generate a negative expansion value. The fixation of the samples for cyclic compression (rheology) experiments (see Fig. 3) was carried out in a way which minimizes contact deformations between the sample and the high-temperature jigs (SiC compression segment and alumina stand). The mentioned undesired deformations occur always as consequence of uneven contact surfaces. In order to obtain even contact surfaces, a sparse layer of alumino-silicate adhesive was applied to the upper and to the lower contact surface of the measured sample. Subsequently, a preload of 10 N was applied to the sample, and it was heated up to 300 °C in the setup employed for the subsequent compression experiment (Fig. 3), at the rate of 5 °C/min. The described procedure led to the hardening of the contact layer between sample and jigs. The surface treatment of the samples was always immediately followed by the rheological experiments at cyclic loading.

All the rheology tests of the high-temperature adhesives were conducted on specimens sized 12 mm × 10 mm × 8 mm which were dried and hardened at room temperature. In the course of the experiments, the temperature was raised from 300 °C to 1000 °C, at a heating rate of 2 °C/min. The experiments were performed on the standard testing machine equipped with a furnace and with a high-temperature compression jig, which had an integrated high-temperature extensometer (Fig. 3).

The typical rheological behaviour of the alumino-silicate adhesives is illustrated in Figs. 6 and 7: The Fig. 7 a displays the detail of one cyclic loading step recorded at the temperatures of 650–658 °C, where the dried adhesive starts to soften. The trapezoidal loading pulse applied by the jigs is plotted as the thin line. The sample deformation caused by this pulse, which is plotted as the thick line, indicates a predominantly viscoelastic behaviour, manifested by a delayed deformation response. Irreversible plastic deformation also takes place, but its exact extent is not evident from the detail shown in Fig. 7a. In the range between 700 and 800 °C, the amplitude of the strain response to loading cycles gradually

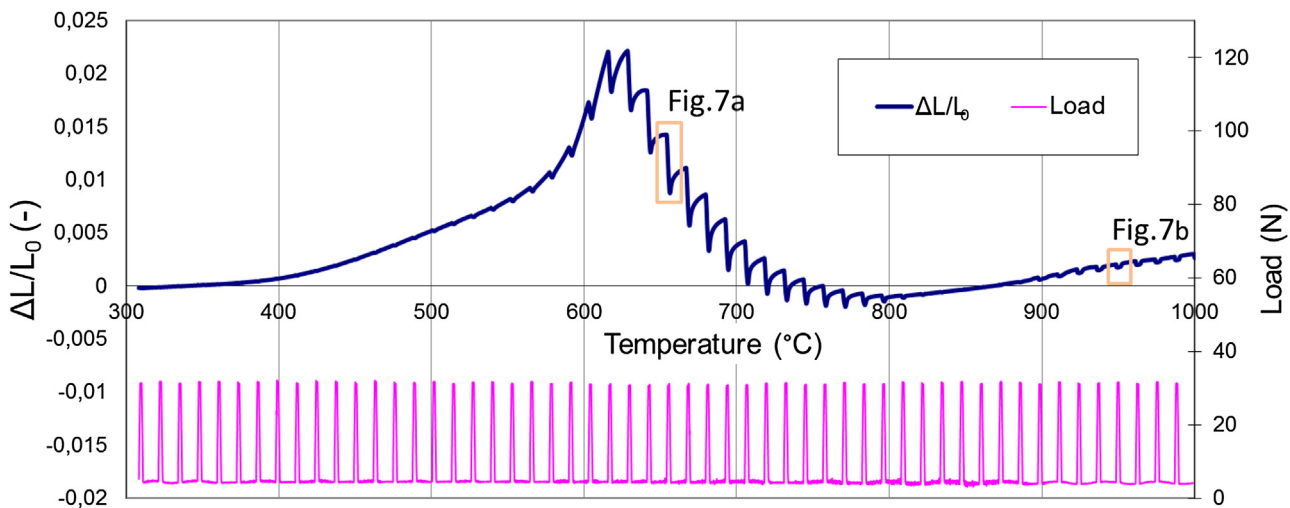


Fig. 6. Experiment studying the rheological and dimensional changes during the high-temperature cure of the alumino-silicate adhesive (material: SA adhesive), by applying cyclic load.

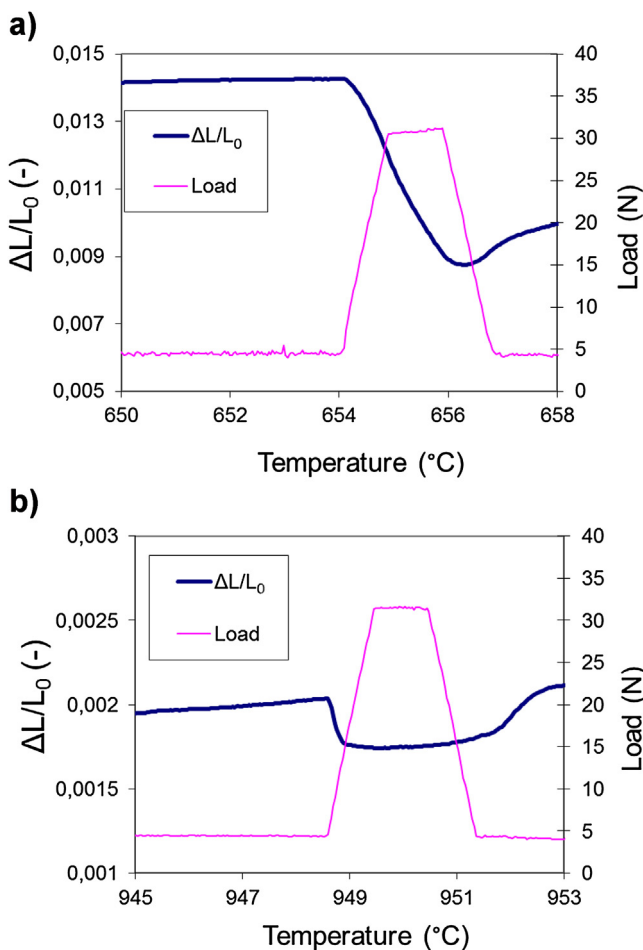


Fig. 7. Detail of one load cycle from Fig. 6: a) cycle at 650 °C; b) cycle at 950 °C.

diminishes until it practically disappears, as consequence of the progressing high-temperature cure of the studied adhesive. The adhesive becomes softer again, if 900 °C are exceeded. Above this temperature, the deformation response has a completely different nature (Fig. 7b), approaching ideal elastic behaviour (only a small viscosity-generated deformation delay is observed).

4.2.2. Viscoelasticity, dimensional changes, and creep effects at high-temperature curing of investigated adhesives

Dilation induced by structural changes which occur during the high temperatures curing of the alumino-silicate adhesives poses a significant problem, because this dilation vastly exceeds the thermal expansion of the stabilized material, and also the creep deformation achievable at temperatures below 680 °C (SA adhesive) or 900 °C (Rk adhesive), as illustrated in Figs. 8 and 9, respectively. Mutual distinction of particular dilation effects and of rheological mechanisms can be done in three experiments, the results of which are shown for the SA adhesive in Fig. 8 and for the Rk adhesive in Fig. 9. The above-described experiment of cyclic loading is plotted with the thin blue line. The bold brown line indicates a similar experiment, i.e. $\Delta L/L_0$ measurement for the adhesive during its cure, but at a constant preload of 5 N instead of cyclic loading. This experiment (brown line) was carried out on adhesives, which were dried and hardened at room temperature, and also the heating rate was the same like in the experiment with the cyclic load. The constant-load-experiment describes the course of dilations associated with the high-temperature curing process, i.e. with irreversible structural changes; the ‘chemical dilations’ are superimposed onto simple thermal dilation of the material. The third experiment, plotted with the yellow line, characterizes the course of the reversible thermal expansion, and was performed under exactly the same thermal and mechanical conditions like the static-load experiment, but on adhesive samples whose structure was fully cured and stabilized by one-hour-annealing at 1000 °C. The course of the dimensional changes of the SA adhesive during its high-temperature cure is shown in Fig. 8. The expansion peak induced by structure changes begins to rise at 430 °C and reaches the maximum value of 1.5% at 623 °C. The magnitude of this expansion vastly exceeds the thermal dilation of the stabilized (cured) SA adhesive, which, in same temperature range, reaches 0.38%. A similar expansion peak was observed in the case of the cure of inorganic adhesives e.g. in [44,45 and 49]. Chang et al. [49] identify the beginning of the peak as a ‘temperature of softening’ and its maximum as the glass transition temperature. Above the temperature of 800 °C, the course of the dilation is nearly identical for the curing and for the thermally stabilized (fully cured) SA adhesive.

The rheological behaviour of the curing SA adhesive has been partly discussed above. Marked is the appearance and prominence of softening, of viscoelastic behaviour, and of creep in the range between 600 and 800 °C. The temperature-dependent viscoelastic deformation can be evaluated as the amplitude of displacement

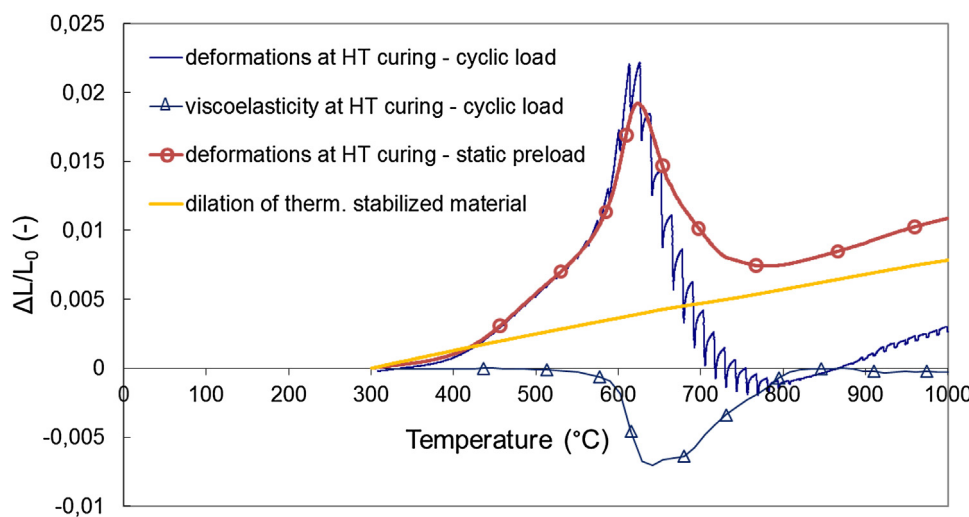


Fig. 8. Rheological behaviour and thermally induced dilations of the SA adhesive.

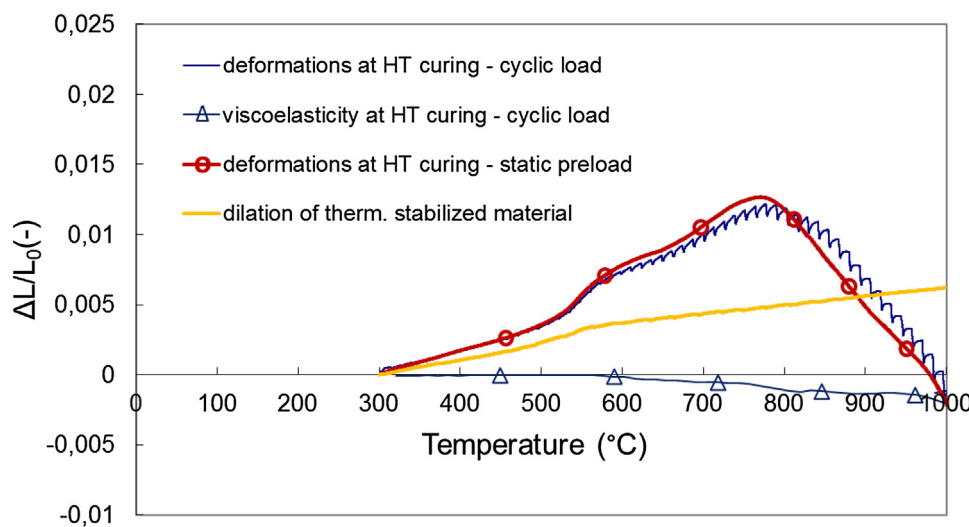


Fig. 9. Rheological behaviour and thermally induced dilations of the Rk adhesive.

achieved during the respective cyclic load. Creep is evident in this temperature range from the difference between the dilation curve recorded under cyclic load and the curve measured with preload. In the case of the first curve, the creep occurs during the particular loading pulses. The accumulated plastic deformation (as result of cyclic loading) reaches approximately 1% at the end of the softening range at ca. 810 °C. The observed plasticity may favourably compensate the internal stresses caused by different dilations of sandwich components during the high-temperature gluing. Between 800 and 900 °C, the SA adhesive does not exhibit any creep or viscoelasticity. The softening which occurs at temperatures above 900 °C is a constant phenomenon, which persists also after full cure (thermal stabilization), and therefore it can have a negative impact in the case of long-term use of the sandwich at high temperatures: A small shear displacement of the skin layers could cause an unacceptably large change in the shape of the sandwich.

Also the Rk adhesive (Fig. 9) exhibits dilations induced by structure changes during its high-temperature cure. The course of these dilations, however, is different from the one observed for the SA adhesive. A distinct onset occurs above 540 °C. The maximum value of 0.7% (after subtraction of thermal expansion) is reached

at 775 °C, i.e. 150 °C higher than in the case of SA. Further temperature increase leads to the shrinkage of the curing Rk sample, and at the temperature of 1000 °C, the sample height is back at the value achieved previously at 300 °C. A favourable property of the Rk adhesive is the relatively low value of the maximum dilation induced by structure changes, which is roughly two times smaller in comparison with SA.

From the rheological viewpoint, the Rk adhesive does not exhibit hardening at higher temperatures, in contrast to SA, which becomes stiff between 800 and 900 °C. The amplitude of the deformation response to cyclic loading begins to be visible above 550 °C, and it uniformly increases up to the end of the experiment at 1000 °C. In comparison with SA, the strain amplitude is lower in the entire temperature range investigated. The deformation mechanism is rather viscoelastic without creep, which becomes evident in view of the almost identical courses of dilation under cyclic load and of dilation with preload. The low ability of the material to deform plastically at the temperatures of maximum structural changes is an adverse property, which could negatively affect the strength of the adhesive joint in a sandwich glued with Rk.

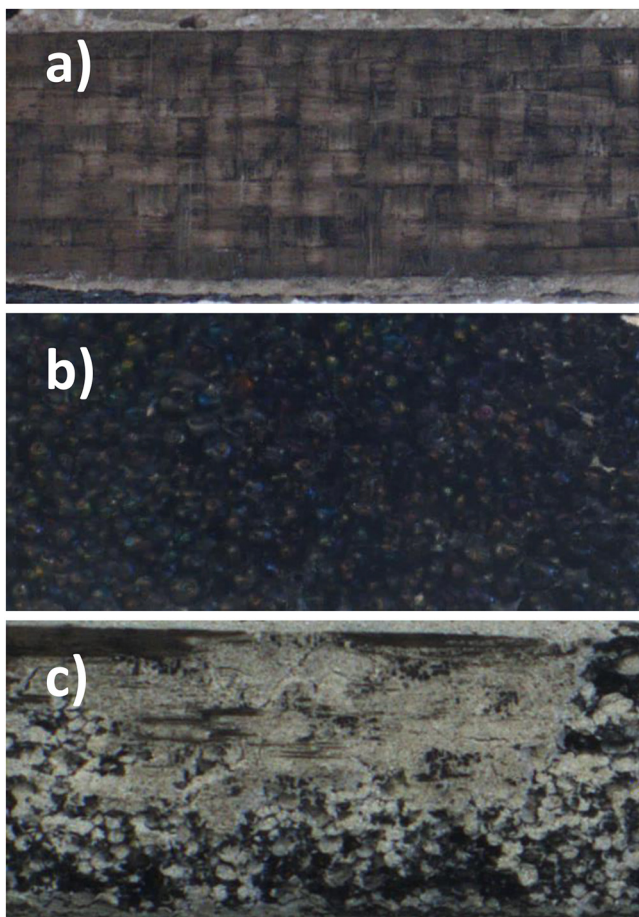


Fig. 10. Examples of fracture types in the prepared sandwiches, differing in fracture location: a) in composite b) in the foam and c) in adhesive.

4.3. Assessment of the quality of the glued joints

The quality of the sandwiches joined by the studied adhesives was experimentally evaluated by means of a modified DCB (Double-Cantilever-Beam) test, which is commonly used for the characterisation of delamination in composites. Additionally, specimens of the sandwiches were also subjected to shear tests. The Fig. 4 shows the experimental setup for both the mentioned tests. The first aim was to identify the weakest place of the tested joint. The recorded load-opening traces were evaluated, and the maximum applied loads, as well as the energies consumed for the formation of new surfaces were determined. The type of fracture was determined by ‘post mortem’ visual evaluation of the broken specimens. Generally, five fracture types (categories) which are identified in view of the fracture location, can be distinguished: i) delamination or fracture within the fibre-reinforced composite skin, i.e. delamination of the composite interlayers, ii) interface fracture going through the composite-adhesive interface, iii) fracture going through the adhesive, iv) interface fracture going through the adhesive-core interface and v) fracture occurring in the ceramic foam core. The last type could be divided into foam fracture close to the joint, and into fracture in the central region of the foam layer. The latter division makes possible to recognize situations, where damage to the foam layer was caused by expansion mismatch (adhesive vs. core) during the heat treatment of the joint. Such a damage predetermines foam cracking near the joint. Examples of the most common fracture types observed in this study are presented in Fig. 10, and they make possible the selection of the combinations of materials which yield the most promising sand-

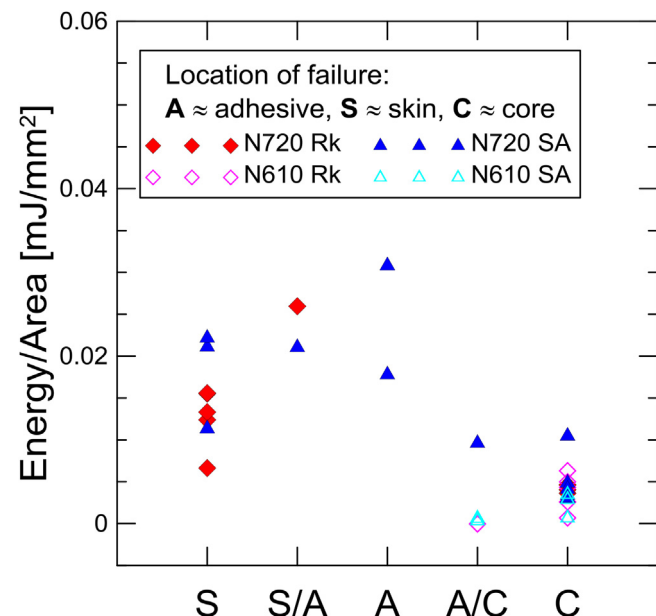


Fig. 11. Results of the DCB test, i.e., normalised work of fracture sorted by fracture location.

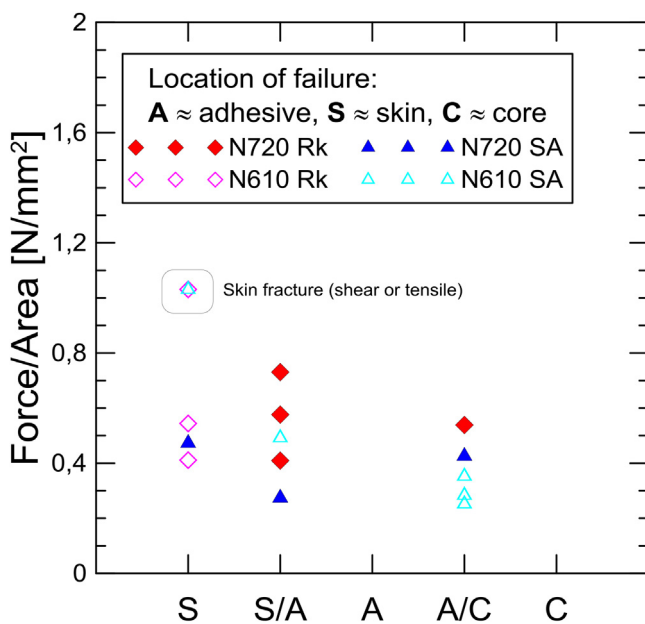
wishes. Generally, it can be seen, that the fracture of the core is the most frequent destruction path if the Rk adhesive in combination with N610 skin is employed. In case of the SA adhesive, the location of the fracture is rather randomly distributed and the fracture process appears to be controlled by location of initial crack-size-defects. Fig. 11 summarises the energy consumption values measured during DCB experiments. The results are sorted to groups which are defined by the location of the fracture. The energy consumed for the formation of new surfaces, i.e. the work of fracture (WoF) normalised by fracture surface was found to be the highest for the fractures which occurred in the joints, and reached its maximum (approximately 0.03 mJ/mm^2) for the fracture going through the adhesive layer. The composite delamination path exhibited twofold lower, but second highest WoF values. Finally, the lowest values (see Fig. 11) were observed for the most frequently occurring fracture type, namely for the one going through the foam. In this latter case, the consumed energy was on the level of 0.004 mJ/mm^2 , which is one order lower than the values obtained if the fracture goes through the adhesive layer.

In the DCB test, the fracture of the sandwich starts from the weakest point (defect), which is usually found in the core layer. In order to more thoroughly evaluate the adhesive efficiency in the sandwich, shear tests were conducted and the obtained results are summarised in Fig. 12, where the normalised de-cohesion force is plotted against the location of the fracture. In this comparison, we can see only negligible differences in the measured force levels. The trend, however, corresponds well with the results plotted in Fig. 11. In some cases, the joint was stronger than the composite itself (note that the de-cohesion forces are only indicative because they are related to joint surface and not to the real fracture surface). Table 2 explains the lower bond strength of the sandwiches based on the N610 composite skin and bonded by the Rk adhesive: For most of these specimens, the fracture damage was localized exclusively in the foam core. This is probably a consequence of curing dilations which damaged the foam core during the high-temperature gluing of the sandwich. This adverse effect was paradoxically supported by the higher interlaminar strength of the N610 composite skin, which led to the rise of higher shear tensions during the gluing process, and as consequence, to a higher damage to the foam core prior to the mechanical tests. On the contrary, the combination of

Table 2

Normalised work of fracture (WoF) and subjective evaluation of failure aspects.

Sandwich composition	Frequency of failure	Average WoF/A (mJ/mm ²)	Adhesion		Core damage	Skin interlayer quality
			adhesive v.s. skin	adhesive v.s. core		
Skin	N720	25%	0.0129 ± 0.0091	very good	very good	low
Adhesive	SA	30%				mediocre
Core	SiOC	45%				
Skin	N720	55%	0.0117 ± 0.0073	very good	very good	low
Adhesive	Rk	10%				mediocre
Core	SiOC	35%				
Skin	N610	0%	0.0020 ± 0.0015	excellent	very good	medium
Adhesive	SA	40%				good
Core	SiOC	60%				
Skin	N610	0%	0.0035 ± 0.0025	excellent	very good	high
Adhesive	Rk	15%				good
Core	SiOC	85%				

**Fig. 12.** Normalized decohesion force obtained from the shear test, sorted by fracture location.

N720 skin, SA adhesive and Si–O–C foam core seems to be the best among the investigated compositions with respect to the reliability and strength of the joint.

5. Conclusions

Both the examined alumino-silicate adhesives, 'SA' and 'Rk', provide for high-quality joints in the studied composite skin/foam core sandwiches, especially in combination with both the examined types of CMC composite skin layer. All the obtained results give a good promise for a long-term use of such joints at high temperatures, including the possibility of cyclic thermal exposure. In the case of the joint of the alumino-silicate adhesives with the Si–O–C foam core of the sandwich, the suitability of this combination was suspected to be more problematic, due to the different thermal expansion of the foam in comparison to the remaining sandwich components. Nevertheless, mechanical tests on sandwich samples indicated a promising potential of the studied materials with the Si–O–C foam core. Important aspects of the preparation of the studied sandwiches were the characteristic distinct dilations,

which resulted from structure changes occurring during the high-temperature cure of both types of the investigated adhesives.

Acknowledgement

This work was financially supported by the Czech Science Foundation project no. GAP107/12/2445 and by the long-term conceptual development of research organization RVO: 67985891. Investigated materials were prepared in cooperation with "Centre for Texture Analysis" funded by the Operational Program Prague—Competitiveness (No.: CZ.2.16/3.1.00/21538).

References

- [1] S. Schmidta, S. Beyera, H. Knabeb, H. Immicha, R. Meistringc, A. Gesslrc, Advanced ceramic matrix composite materials for current and future propulsion technology applications, *Acta Astronaut.* 55 (2004) 409–420.
- [2] Y. Li, J.B. Li, R. Zhang, Energy-absorption performance of porous materials in sandwich composites under hypervelocity impact loading, *Compos. Struct.* 64 (2004) 71–78.
- [3] H.N.G. Wadley, M.R. O'Masta, K.P. Dharmasena, B.G. Compton, E.A. Gamble, F.W. Zok, Effect of core topology on projectile penetration in hybrid aluminum/alumina sandwich structures, *Int. J. Impact Eng.* 62 (2013) 99–113.
- [4] N.P. Bansal, Mechanical behavior of silicon carbide fiber-reinforced strontium aluminosilicate glass-ceramic composites, *Mater. Sci. Eng. A* 231 (1997) 117–127.
- [5] R.E. Tressler, Recent developments in fibers and interphases for high temperature ceramic matrix composites, *Compos. A: Appl. Sci. Manuf.* 30 (1999) 429–437.
- [6] B. Wilshire, F. Carreño, Deformation and damage processes during tensile creep of ceramic-fibre-reinforced ceramic-matrix composites, *J. Eur. Ceram. Soc.* 20 (2000) 463–472.
- [7] A. Yousefpour, M.N.G. Nejad, Processing and performance of Nicalon/Blackglas and Nextel/Blackglas using cure-on-the-fly filament winding and preceramic polymer pyrolysis with inactive fillers, *Compos. Sci. Technol.* 61 (2001) 1813–1820.
- [8] B. Wilshire, Creep property comparisons for ceramic-fibre-reinforced ceramic-matrix composites, *J. Eur. Ceram. Soc.* 22 (2002) 1329–1337.
- [9] J.L. Chermanta, G. Boitierb, S. Darzensa, G. Farizya, J. Vicensa, J.C. Sangleboeuf, The creep mechanism of ceramic matrix composites at lowtemperature and stress, by a material science approach, *J. Eur. Ceram. Soc.* 22 (2002) 2443–2460.
- [10] M. Černý, P. Glogar, Z. Sucharda, et al., Properties and performance of polysiloxane-derived ceramic matrix in heat resistant composites reinforced with R-glass or fine ceramic fibres, *Ceram. Silik.* 49 (3) (2005) 145–152.
- [11] M. Černý, P. Glogar, Z. Sucharda, Mechanical properties of basalt fiber reinforced composites prepared by partial pyrolysis of a polymer precursor, *J. Compos. Mater.* 43 (9) (2009) 1109–1120.
- [12] D. Koch, K. Tushnev, G. Grathwohl, Ceramic fiber composites: experimental analysis and modeling of mechanical properties, *Compos. Sci. Technol.* 68 (2008) 1165–1172.
- [13] S.H. Lee, M. Weinmann, Cfiber/SiCfiller/Si–B–C–Nmatrix composites with extremely high thermal stability, *Acta Mater.* 57 (2009) 4374–4381.
- [14] M. Černý, A. Strachota, Z. Chlup, Z. Sucharda, M. Zaloudkova, P. Glogar, Ivo Kubena, Strength, elasticity and failure of composites with pyrolyzed matrices based on polymethylsiloxane resins with optimized ratio of D and T components, *J. Compos. Mater.* 47 (8) (2013) 1055–1066.

- [15] T.P. Coons, J.W. Reutenaer, A. Mercado, M.A. Kmetz, S.L. Suib, The characterization of an oxide interfacial coating for ceramic matrix composites, *Mater. Sci. Eng. A* 573 (2013) 190–196.
- [16] C. Cluzel, E. Baranger, P. Ladèvèze, A. Mouret, Mechanical behaviour and lifetime modelling of self-healing ceramic-matrix composites subjected to thermomechanical loading in air, *Compos. A: Appl. Sci. Manuf.* 40 (2009) 976–984.
- [17] R.M. Sullivan, Time-dependent stress rupture strength of Hi-Nicalonfiber-reinforced silicon carbide composites at intermediate temperatures, *J. Eur. Ceram. Soc.* 36 (2016) 1885–1892.
- [18] T. Takahashi, H. Münstedt, M. Modesti, P. Colombo, Oxidation resistant ceramic foam from a silicone preceramic polymer/polyurethane blend, *J. Eur. Ceram. Soc.* 21 (2001) 2821–2828.
- [19] P. Colombo, E. Bernardo, Macro- and micro-cellular porous ceramics from preceramic polymers, *Compos. Sci. Technol.* 63 (2003) 2353–2359.
- [20] F.A. Costa Oliveira, S. Dias, M. Fátima Vaz, J. Cruz Fernandes, Behaviour of open-cell cordierite foams under compression, *J. Eur. Ceram. Soc.* 26 (2006) 179–186.
- [21] L. Yin, H.X. Peng, S. Dhara, L. Yang, B. Su, Natural additives in protein coagulation casting process for improved microstructural controllability of cellular ceramics, *Compos. B: Eng.* 40 (2009) 638–644.
- [22] C. D'Angelo, A. Ortona, P. Colombo, Influence of the loading direction on the mechanical behavior of ceramic foams and lattices under compression, *Acta Mater.* 61 (2013) 5525–5534.
- [23] L. Fiocco, H. Elsayeda, J.K.M.F. Daguanob, V.O. Soares, E. Bernardo, Silicone, resinsmixed with active oxide fillers and Ca-Mg Silicate glass asalternative/integrative precursors for wollastonite-diopside glass-ceramic foams, *J. Non-Cryst. Solids* 416 (2015) 44–49.
- [24] B. Man, Y. Lin, G. Liu, D. Liang, Preparation and properties of Al_2O_3 - MgAl_2O_4 ceramic foams, *Ceram. Int.* 41 (2015) 3237–3244.
- [25] Adhimoolam Bakthavachalam Kousaalya, Ravi Kumar, B.T.N. Sridhar, Thermal conductivity of precursor derived Si–B–C–N ceramic foams using Metroxylon sagu as sacrificial template, *Ceram. Int.* 41 (2015) 1163–1170.
- [26] Z. Chlup, M. Černý, A. Strachota, J. Svítílová, M. Halasová, Effect of ageing at 1200 °C in oxidative environment on the mechanical response of SiOC foams, *Ceram. Int.* 41 (2015) 9030–9034.
- [27] Mengguang Zhu, Ru Ji, Zhongmin Li, Hao Wang, LiLi Liu, Zuotai Zhang, Preparation of glass ceramic foams for thermal insulation applications from coal fly ash and waste glass, *Constr. Build. Mater.* 112 (2016) 398–405.
- [28] M. Černý, Z. Chlup, A. Strachota, J. Svítílová, J. Schweigstillova, M. Halasova, S. Ryglova, Si–O–C ceramic foams derived from polymethylphenylsiloxane precursor with starch as foaming agent, *J. Eur. Ceram. Soc.* 35 (2015) 3427–3436.
- [29] S. Tripathy, D.S. Saini, D. Bhattacharya, Synthesis and fabrication of MgAl_2O_4 ceramic foam via a simple, low-cost and eco-friendly method, *J. Asian Ceram. Soc.* 4 (2016) 149–154.
- [30] L. Fiocco, L. Ferroni, C. Gardin, B. Zavan, M. Secco, S. Matthews, E. Bernardo, Wollastonite-diopside glass-ceramic foams from supercritical carbon dioxide-assisted extrusion of a silicone resin and inorganic fillers, *J. Non-Cryst. Solids* 443 (2016) 33–38.
- [31] A. Strachota, M. Černý, Z. Chlup, K. Rodzen, K. Depa, M. Halasova, M. Slouf, J. Schweigstillova, Preparation of finely macroporous SiOC foams with high mechanical properties and with hierarchical porosity via pyrolysis of a siloxane/epoxide composite, *Ceram. Int.* 41 (2015) 8402–8410.
- [32] O. Lyckfeldt, J.M.F. Ferreira, Processing of porous ceramics by 'starch consolidation', *J. Eur. Ceram. Soc.* 18 (1998) 131–140.
- [33] E. Gregorova, W. Pabst, Porosity and pore size control in starch consolidation casting of oxide ceramics—achievements and problems, *J. Eur. Ceram. Soc.* 27 (2007) 669–672.
- [34] Z. Živcová, M. Černý, W. Pabst, E. Gregorova, Elastic properties of porous oxide ceramics prepared using starch as a pore-forming agent, *J. Eur. Ceram. Soc.* 29 (2009) 2765–2771.
- [35] Eva Gregorová, Willi Pabst, Zuzana Živcová, Ivona Sedlářová, Svatava Holíková, Porous alumina ceramics prepared with wheat flour, *J. Eur. Ceram. Soc.* 30 (2010) 2871–2880.
- [36] E. Gregorová, W. Pabst, Process control and optimized preparation of porous alumina ceramics by starch consolidation casting, *J. Eur. Ceram. Soc.* 31 (2011) 2073–2081.
- [37] M.H. Talou, M.A. Camerucci, Processing of porous mullite ceramics using novel routes by starch consolidation casting, *J. Eur. Ceram. Soc.* 35 (2015) 1021–1030.
- [38] K. Wei, R. He, X. Cheng, R. Zhang, Y. Pei, D. Fang, Fabrication and mechanical properties of lightweight ZrO_2 ceramic corrugated core sandwich panels, *Mater. Des.* 64 (2014) 91–95.
- [39] X. Zhang, K. Yu, Y. Bai, R. Zhao, Thermal vibration characteristics of fiber-reinforced mullite sandwich structure with ceramic foams core, *Compos. Struct.* 131 (2015) 99–106.
- [40] Xiao-zhou Wang, Jun Wang, Hao Wang, Preparation and performance of a heat-resistant organic adhesive obtained via a liquid SiC precursor, *Int. J. Adhes. Adhes.* 35 (2012) 17–20.
- [41] Xiaozhou Wang, Jun Wang, Hao Wang, Preparation of high-temperature organic adhesives and their performance for joining SiC ceramic, *Ceram. Int.* 39 (2013) 1365–1370.
- [42] Yan Qin, Zhilong Rao, Zhixiong Huang, Hui Zhang, Jinrong Jia, Fuzhong Wang, Preparation and performance of ceramizable heat-resistant organic adhesive for joining Al_2O_3 ceramics, *Int. J. Adhes. Adhes.* 55 (2014) 132–138.
- [43] Xiaozhou Wang, Jun Wang, Hao Wang, Performance and structural evolution of high-temperature organic adhesive for joining Al_2O_3 ceramics, *Int. J. Adhes. Adhes.* 45 (2013) 1–6.
- [44] K.D. Meinhardt, D.-S. Kim, Y.-S. Chou, K.S. Weil, Synthesis and properties of a barium aluminosilicate solid oxide fuel cell glass-ceramic sealant, *J. Power Sources* 182 (2008) 188–196.
- [45] Hsiu-Tao Chang, Chih-Kuang Lin, Chien-Kuo Liu, High-temperature mechanical properties of a glass sealant for solid oxide fuel cell, *J. Power Sources* 189 (2009) 1093–1099.
- [46] E.V. Stephens, J.S. Vetrano, B.J. Koeppl, Y. Chou, X. Sun, M.A. Khaleel, Experimental characterization of glass-ceramic seal properties and their constitutive implementation in solid oxide fuel cell stack models, *J. Power Sources* 193 (2009) 625–631.
- [47] J. Milhans, S. Ahz, H. Garmestani, M.A. Khaleel, X. Sun, B.J. Koeppl, Modeling of the effective elastic and thermal properties of glass-ceramic solid oxide fuel cell seal materials, *Mater. Des.* 30 (2009) 1667–1673.
- [48] N. Govindarajua, W.N. Liub, X. Sunb, P. Singhb, R.N. Singh, A modeling study on the thermomechanical behavior of glass-ceramic and self-healing glass seals at elevated temperatures, *J. Power Sources* 190 (2009) 476–484.
- [49] Hsiu-Tao Chang, Chih-Kuang Lin, Chien-Kuo Liu, Effects of crystallization on the high-temperature mechanical properties of a glass sealant for solid oxide fuel cell, *J. Power Sources* 195 (2010) 3159–3165.
- [50] J. Milhans, D. Li, M. Khaleel, X. Sun, H. Garmestani, Statistical continuum mechanics analysis of effective elastic properties in solid oxide fuel cell glass-ceramic seal material, *J. Power Sources* 195 (2010) 5726–5730.
- [51] J. Milhans, M. Khaleel, X. Sun, M. Tehrani, M. Al-Haik, H. Garmestani, Creep properties of solid oxide fuel cell glass-ceramic seal G18, *J. Power Sources* 195 (2010) 3631–3635.
- [52] L. Blum, S.M. Groß, J. Malzbender, U. Pabst, M. Peksen, R. Peters, I.C. Vinke, Investigation of solid oxide fuel cell sealing behavior under stack relevant conditions at Forschungszentrum Jülich, *J. Power Sources* 196 (2011) 7175–7181.
- [53] J. Milhans, D.S. Li, M. Khaleel, X. Sun, H. Garmestani, Prediction of the effective coefficient of thermal expansion of heterogeneous media using two-point correlation functions, *J. Power Sources* 196 (2011) 3846–3850.
- [54] J. Milhans, D.S. Li, M. Khaleel, X. Sun, Marwan S. Al-Haik, Adrian Harris, H. Garmestani, Mechanical properties of solid oxide fuel cell glass-ceramic seal at high temperatures, *J. Power Sources* 196 (2011) 5599–5603.
- [55] Hsiu-Tao Chang, Chih-Kuang Lin, Chien-Kuo Liu, Szu-Han Wu, High-temperature mechanical properties of a solid oxide fuel cell glass sealant in sintered forms, *J. Power Sources* 196 (2011) 3583–3591.
- [56] Wei Xu, Xin Sun, Elizabeth Stephens, Ioannis Mastorakos, Mohammad A. Khaleel, Hussein Zbib, A mechanistic-based healing model for self-healing glass seals used in solid oxide fuel cells, *J. Power Sources* 218 (2012) 445–454.
- [57] L. Di Felice, V. Middelkoop, V. Anzoletti, F. Snijkers, M. van Sint Annaland, F. Gallucci, New high temperature sealing technique and permeability data for hollow fiber BSCF perovskite membranes, *Chem. Eng. Process.* 107 (2014), <http://dx.doi.org/10.1016/j.cep.2014.12.004>.
- [58] M. Černý, Z. Chlup, A. Strachota, M. Halasova, S. Ryglova, Jana Schweigstillova, J. Svítílová, M. Havelcová, Changes in structure and in mechanical properties during the pyrolysis conversion of crosslinked polymethylphenylsiloxane and polymethylphenylsiloxane resins to silicon oxycarbide glass, *Ceram. Int.* 41 (2015) 6237–6247.
- [59] M. Halasova, Z. Chlup, A. Strachota, et al., Mechanical response of novel SiOC glasses to high temperature exposition, *J. Eur. Ceram. Soc.* 32 (2012) 4489–4495.